The fracture toughness of demi-regular lattices

Milad Omidi, Luc St-Pierre*

Department of Mechanical Engineering, Aalto University, Espoo 02150, Finland

Abstract

The properties of lattice materials are strongly influenced by their nodal connectivity; yet, previous studies have focused mainly on topologies with a single vertex configuration. This work investigates the potential of demi-regular lattices, with two vertex configurations, to outperform existing topologies, such as triangular and kagome lattices. We used finite element simulations to predict the fracture toughness of three elastic-brittle demi-regular lattices under mode I, mode II, and mixed-mode loading conditions. The fracture toughness of two demi-regular lattices scales linearly with relative density $\bar{\rho}$, and outperform a triangular lattice by 15% under mode I and 30% under mode II. Their mixed-mode fracture envelopes are also up to 43% larger than that of a triangular lattice. The third demi-regular lattice has a fracture toughness that scales with $\sqrt{\bar{\rho}}$ and matches the remarkable toughness of a kagome lattice. These findings open new avenues for the development of tougher lightweight materials.

Keywords: Cellular materials, Fracture, Toughness, Finite element analysis, Demi-regular tessellations

Lattice materials are well known for their ability to be stiff and strong at low densities [1–6], but their architecture can also be tailored to achieve a high fracture toughness [7–10]. While the stiffness and strength of lattices are limited by bounds, and architectures approaching those limits have been identified [11–13], their fracture toughness is not theoretically bounded. Relatively few topologies have been investigated so far in the quest to maximise fracture toughness; therefore, the aim of this study is to discover tougher lattice materials by exploring novel architectures.

The influence of topology on fracture toughness has been documented predominantly for

*Corresponding author: luc.st-pierre@aalto.fi

Table 1: Constants D_I, D_{II}, and d in (1) for planar transversely isotropic lattice materials. These topologies are shown in Fig. 1 and 2.

Topology	D_I	D_{II}	d	Reference
Hexagonal	0.800	0.370	2	[19]
Triangular	0.500	0.380	1	[19]
Snub-trihexagonal	0.460	—	1	[31]
Kagome	0.212	0.133	0.5	[19]
A	0.570	0.510	1	This study
B	0.580	0.490	1	This study
C	0.210	0.150	0.5	This study

planar lattices. Analytical [14–18], numerical [19–25] and experimental [26–29] studies have shown that the fracture toughness of an elastic-brittle lattice can be expressed as:

$$\frac{K_{Ic}}{\sigma_{ts}\sqrt{\ell}} = D_I \bar{\rho}^d \qquad \text{and} \qquad \frac{K_{IIc}}{\sigma_{ts}\sqrt{\ell}} = D_{II} \bar{\rho}^d, \tag{1}$$

where K_{Ic} and K_{IIc} are the fracture toughness under mode I and II, respectively; $\bar{\rho}$ is the relative density of the lattice; ℓ is the length of the cell walls; σ_{ts} is the tensile strength of the parent material; and the constants D_I, D_{II}, and d are given in Table 1 for planar transversely isotropic lattices, which are shown in Fig. 1. Orthotropic topologies, such as the square or snub-square lattices, have also been investigated but they do not outperform the toughest isotropic lattices [20, 21, 27, 30, 31].

The exponent d has a strong effect on the fracture toughness: a lower d leads to a higher fracture toughness at low relative densities $\bar{\rho}$, see (1). The exponent d is insensitive to the choice of parent material [32], and strongly influenced by the lattice's nodal connectivity (the number of bars meeting at each joint). With three bars per joint, the hexagonal lattice (Fig. 1a) deforms by bending, and this leads to a particularly low fracture toughness with $d = 2$ [14, 15, 33, 34]. In contrast, the triangular lattice (Fig. 1b), with six bars per joint, and the snub-trihexagonal architecture (Fig. 1c), with five bars per joint, are stretching-dominated meaning that their members carry predominantly axial stresses. This mode of deformation leads to a fracture toughness that scales linearly with relative density, with an exponent

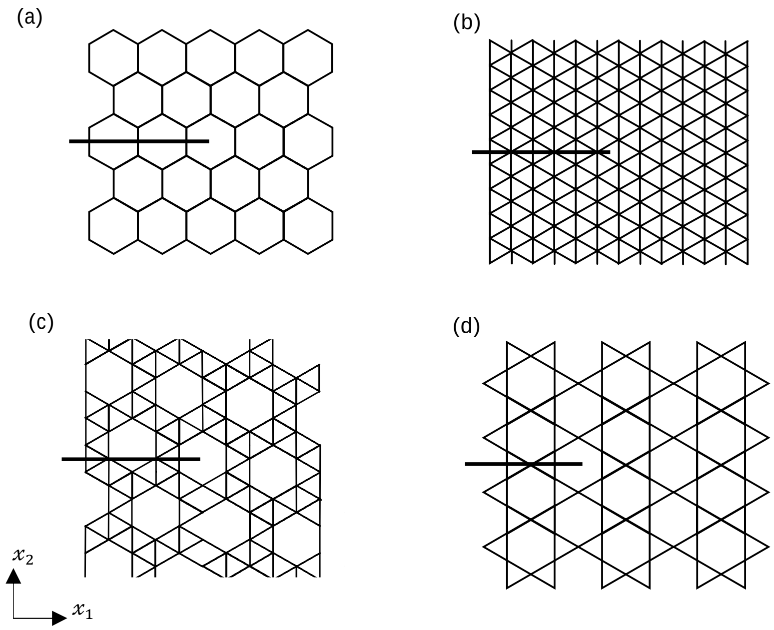

Figure 1: Four planar topologies listed in Table 1: (a) hexagonal, (b) triangular, (c) snub-trihexagonal, and (d) kagome lattices. In all cases, the thick black line denotes the position of the initial crack considered in previous studies [19, 31].

$d = 1$ [19, 31, 35]. Finally, the kagome lattice (Fig. 1d), with four bars per joint, has an unusual behaviour. It is stretching-dominated, as stiff and strong as a triangular lattice [2], but its fracture toughness scales with the square-root of relative density ($d = 0.5$), making it remarkably tough at low values of $\bar{\rho}$. This exceptional toughness is due to a crack tip blunting phenomenon caused by localised bending deformation [19, 32]. The kagome lattice is the only known topology with $d = 0.5$, and it is unclear if other architectures could match or exceed its toughness.

All architectures investigated so far share a similar characteristic: they have a unique vertex configuration. This means that each vertex inside a given lattice is surrounded by the same sequence of polygons, see Fig. 1. This is an important limitation considering that nodal connectivity has such a strong effect on fracture toughness. To broaden the search for tougher architectures, we turn our attention to demi-regular lattices, which have two different vertex configurations. Three examples are shown in Fig. 2: demi-regular lattices A and B have joints with five and others with six bars, whereas the vertices of tessellation C have either four or five struts. These three demi-regular lattices were recently shown to be

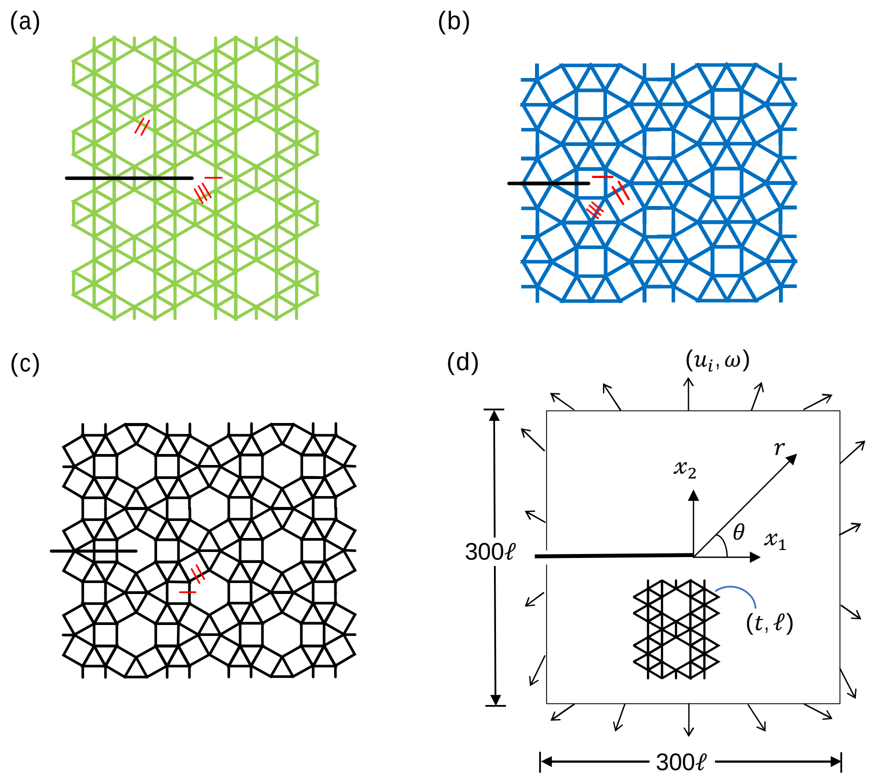

Figure 2: Demi-regular lattices (a) A, (b) B, and (c) C. The thick black line indicates the position of the initial crack, and fracture sites under mixed-mode loading are shown with |, ||, and ||| symbols. (d) Domain and coordinate system used in our finite element predictions.

stretching-dominated and transversely isotropic, with an elastic modulus that is comparable but slightly lower than that of kagome and triangular lattices [36]. The aim of this study is to characterise the fracture behaviour of these three demi-regular lattices and evaluate if they are tougher than other stretching-dominated architectures, such as kagome and triangular lattices.

The fracture toughness of each demi-regular lattice was predicted using Finite Element (FE) simulations; more specifically, with the static implicit solver of the commercial software Abaqus. Our modelling approach relied on the boundary layer method, as used in previous studies [19, 21, 31, 34, 35], to ensure that our results can be compared directly those in Table 1.

For each demi-regular lattice, a large square domain was created with a side length of 300ℓ, where ℓ is the length of a cell wall (see Fig. 2d). This domain included a semi-infinite crack along the negative x_1 axis and a detailed view showing the position of the crack tip for each topology is given in Fig. 2. Numerical experimentation showed that moving the crack tip to another cell or changing the crack orientation have a negligible effect on the fracture toughness. We show, in supplementary material, that the crack orientation considered in Fig. 2 is the one associated with the lowest mode I fracture toughness.

The cell walls were meshed using Timoshenko beam elements (B21 in Abaqus notation). A fine mesh size of $\ell/30$ was used within a $60\ell \times 60\ell$ area centered at the crack tip, whereas a coarser mesh size of $\ell/10$ was employed elsewhere. Further mesh refinements had an imperceptible effect on the results. The relative density $\bar{\rho}$ was varied from 0.01 to 0.2 by changing the strut thickness t while keeping the strut length ℓ fixed. The relationship between $\bar{\rho}$ and t/ℓ is given in supplementary material for each demi-regular lattice.

Each node on the domain's perimeter was subjected to a displacement corresponding to the asymptotic crack tip solution from linear elastic fracture mechanics. The displacement field included two translations, u_1 and u_2, and an in-plane rotation ω, see Fig. 2d. Expressions for u_1, u_2, and ω are lengthy and provided in supplementary material. They are functions of the nodal coordinates (r, θ); the elastic properties of the lattice given in [36]; and the applied stress intensify factors K_I and K_{II} for modes I and II, respectively. Our approach is identical to that used by Fleck and Qiu [19] to predict the fracture toughness of other planar transversely isotropic lattices.

The cell walls were modeled as an elastic-brittle material, characterised by a Young's modulus E_s and Poisson ratio ν_s, up to a tensile fracture strength σ_{ts}. In our simulations, the fracture toughness K_{Ic} (or K_{IIc}) corresponded to the value of K_I (or K_{II}) when the maximum tensile stress in any element of the lattice reached the strength of the parent material σ_{ts}.

The fracture toughness of each demi-regular lattice is plotted as a function of relative density in Fig. 3a for mode I and Fig. 3b for mode II. In each plot, the fracture toughness is normalised by $\sigma_{ts}\sqrt{\ell}$ based on the scaling law given in (1). Deformed meshes for each topology with $\bar{\rho} = 0.05$ are given in Fig. 4 for both modes I and II.

The fracture toughness of demi-regular lattices A and B scales linearly with relative density, see Fig. 3, corresponding to an exponent $d = 1$ in (1). In contrast, the fracture toughness of tessellation C scales with $\sqrt{\bar{\rho}}$, giving $d = 0.5$. With a lower value of d, lattice C

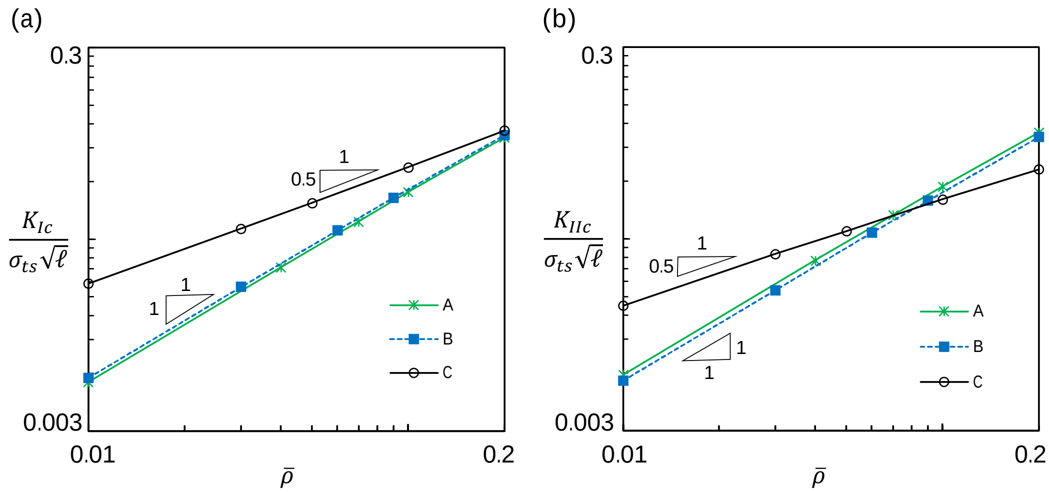

Figure 3: Fracture toughness under (a) mode I and (b) mode II, as a function of relative density $\bar{\rho}$. Results are given for demi-regular lattices A, B, and C.

is significantly tougher than topologies A and B at low relative densities. This holds true for both K_{Ic} and K_{IIc} as the exponent d is the same for both modes I and II. The lower value of d for topology C is due to crack tip blunting, which does not occur in tessellations A and B, see Fig. 4.

The results in Fig. 3 were used to evaluate the constants D_I and D_{II} in (1) and their values are given in Table 1. For each demi-regular lattice, $D_I > D_{II}$ meaning that fracture toughness is higher for mode I than mode II. The differences are, however, sensitive to topology; the ratios K_{Ic}/K_{IIc} are 1.12, 1.18 and 1.40 for tessellations A, B, and C, respectively.

The fracture envelope under mixed-mode loading is plotted in Fig. 5a for demi-regular lattices A and B, and in Fig. 5b for tessellation C. Based on the results in Fig. 3, the stress intensity factors K_I and K_{II} are normalised here by $\sigma_{ts}\bar{\rho}\sqrt{\ell}$ for lattices A and B, and by $\sigma_{ts}\sqrt{\bar{\rho}\ell}$ for tessellation C. This normalisation ensures that each fracture envelope is independent of relative density $\bar{\rho}$. Each envelope is formed by two or three straight lines, where each segment corresponds to a different fracture location. The segments are labeled |, ||, and ||| in Fig. 5, and the corresponding fracture locations are shown in Fig. 2.

The fracture envelopes of lattices A and B are close to a quarter circle, whereas that of tessellation C has two straight sides, see Fig. 5. For topologies A and B, fracture takes place in the vertical bar in front of the crack tip when $K_I \gg K_{II}$ and moves off the crack plane

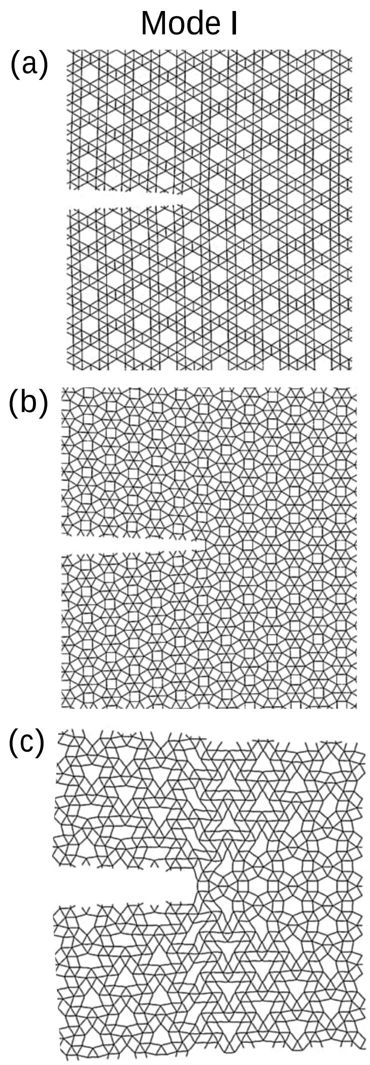

Figure 4: Deformed meshes for demi-regular lattices (a) A, (b) B, and (c) C. Results are shown for mode I (left) and mode II (right) loading. All lattices have a relative density $\bar{\rho} = 0.05$.

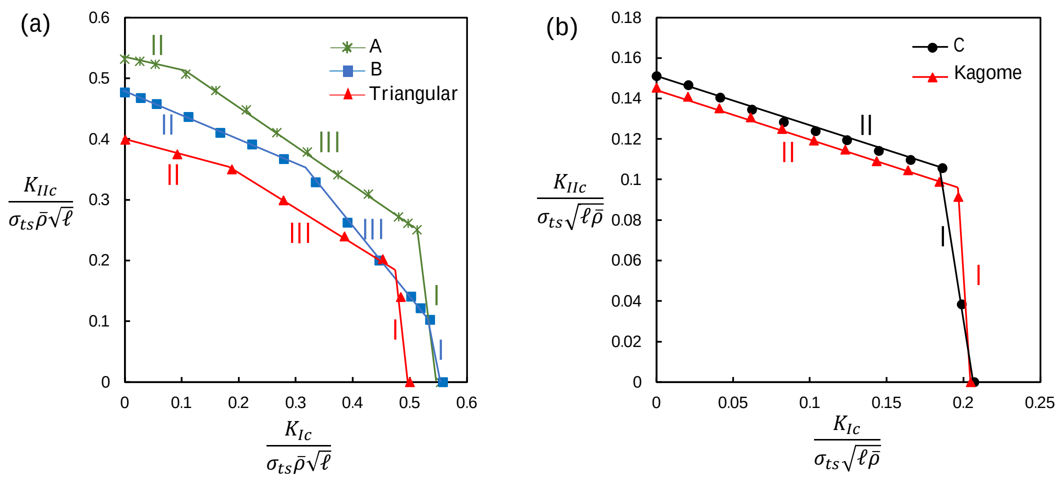

Figure 5: Mixed-mode fracture envelopes: (a) demi-regular lattices A and B are compared to a triangular tessellation and (b) demi-regular lattice C is compared to a kagome tessellation. The segments labelled |, ||, and ||| correspond to different fracture sites, which are shown in Fig. 2.

when K_{II} increases, see Fig. 2. In contrast, the fracture sites in tessellation C are always off the crack plane and located a few cells away from the crack tip.

The fracture behaviour of demi-regular lattices A and B is very similar to that of a triangular lattice. These three topologies have a fracture toughness that scales linearly with relative density ($d = 1$), see Fig. 3 and [19]. The bars in a triangular lattice carry high axial stresses and minimal bending stresses [19], and we noticed the same for demi-regular lattices A and B. This is characteristic of lattices with a high nodal connectivity: tessellations A and B have either five or six bars per vertex, and similarly, a triangular lattice has six. Lastly, the fracture sites in a triangular lattice are close to the crack tip (typically within in a distance ℓ) [19], and we observed the same for tessellations A and B, see Fig. 2a,b.

In contrast, demi-regular lattice C behaves similarly to a kagome lattice since their fracture toughness scales with the square-root of relative density ($d = 0.5$), see Fig. 3 and [19]. The high fracture toughness of the kagome lattice is attributed to elastic crack tip blunting, characterised by bands of bending deformation near the crack tip [19]. The same phenomenon is observed in demi-regular lattice C, see Fig. 4c. The fracture sites in a kagome lattice are located at a distance of $\approx 3\ell$ from the crack tip [19], and tessellation C exhibit the same feature, see Fig 2c. Finally, both topologies have a similar nodal connectivity: topology C has four or five bars per joint, whereas the kagome lattice has four.

Based on the similarities detailed above, it is justified to compare the performances of demi-regular lattices A and B to those of a triangular lattice; and those of tessellation C to a kagome lattice. Their constants D_I and D_{II} are compared in Table 1, and their fracture envelopes are contrasted in Fig. 5. Here, the envelopes for triangular and kagome lattices were obtained following the same modelling approach detailed above and their orientations are given in Fig. 1.

The performances of demi-regular lattice C are very similar to those of a kagome lattice; they have practically the same fracture toughness, see Table 1, and fracture envelope under mixed-mode loading, see Fig. 5b. Otherwise, demi-regular lattices A and B are both tougher than a triangular lattice. Tessellations A and B have a similar fracture toughness, which is roughly 15% tougher than a triangular lattice under mode I, and approximately 30% tougher in mode II, see Table 1. Demi-regular lattices A and B also outperform the triangular lattice under mixed-mode loading, see Fig. 5a. Quantitatively, the area contained within the fracture envelope of tessellation A is 43% larger than that of a triangular lattice.

In summary, we showed that three previously unexplored demi-regular lattices have a remarkably high fracture toughness. Demi-regular lattices A and B have a fracture toughness that scales linearly with relative density and are tougher than a triangular lattice under mode I, mode II, and mixed-mode loading conditions. Previously, the kagome lattice was the only known topology with a fracture toughness that scales with the square-root of relative density. We discovered that demi-regular lattice C exhibit the same scaling, and has a fracture toughness equal to that of a kagome lattice. While these results are step forward in the development of tougher lightweight materials, future work is needed to evaluate the imperfection sensitivity of these three demi-regular lattices. The fracture toughness of the kagome lattice is highly imperfection sensitive [21], but we anticipate that demi-regular lattice C, with a slightly higher nodal connectivity, will be more tolerant to imperfections.

Acknowledgements

This work was supported by the Academy of Finland (grant 322007).

Supplementary material

Supplementary material related to this article can be found online.

References

[1] N. A. Fleck, V. S. Deshpande, M. F. Ashby, Micro-architectured materials: past, present and future, Proc. R. Soc. A: Math. Phys. Eng. Sci. 466 (2010) 2495–2516.

[2] A.-J. Wang, D. L. McDowell, In-plane stiffness and yield strength of periodic metal honeycombs, J. Eng. Mater. Technol. 126 (2004) 137–156.

[3] M. Omidi, L. St-Pierre, Mechanical properties of semi-regular lattices, Mater. Des. 213 (2022) 110324.

[4] S. Torquato, L. V. Gibiansky, M. J. Silva, L. J. Gibson, Effective mechanical and transport properties of cellular solids, Int. J. Mech. Sci. 40 (1998) 71–82.

[5] F. Côté, V. S. Deshpande, N. A. Fleck, A. G. Evans, The compressive and shear responses of corrugated and diamond lattice materials, Int. J. Solids Struct. 43 (2006) 6220–6242.

[6] A. Markou, L. St-Pierre, A novel parameter to tailor the properties of prismatic lattice materials, Int. J. Mech. Sci. 219 (2022) 107079.

[7] M. R. O'Masta, L. Dong, L. St-Pierre, H. N. Wadley, V. S. Deshpande, The fracture toughness of octet-truss lattices, J. Mech. Phys. Solids 98 (2017) 271–289.

[8] H. Gu, S. Li, M. Pavier, M. M. Attallah, C. Paraskevoulakos, A. Shterenlikht, Fracture of three-dimensional lattices manufactured by selective laser melting, Int. J. Solids Struct. 180-181 (2019) 147–159.

[9] Y. Liu, L. St-Pierre, N. A. Fleck, V. S. Deshpande, A. Srivastava, High fracture toughness micro-architectured materials, J. Mech. Phys. Solids 143 (2020) 104060.

[10] A. J. D. Shaikeea, H. Cui, M. O'Masta, X. R. Zheng, V. S. Deshpande, The toughness of mechanical metamaterials, Nat. Mater. 21 (2022) 297—304.

[11] J. B. Berger, H. N. G. Wadley, R. M. McMeeking, Mechanical metamaterials at the theoretical limit of isotropic elastic stiffness, Nature 543 (2017) 533–537.

[12] T. Tancogne-Dejean, M. Diamantopoulou, M. B. Gorji, C. Bonatti, D. Mohr, Metamaterials: 3D plate-lattices: an emerging class of low-density metamaterial exhibiting optimal isotropic stiffness, Adv. Mater. 30 (2018) 1870337.

[13] M. T. Hsieh, B. Endo, Y. Zhang, J. Bauer, L. Valdevit, The mechanical response of cellular materials with spinodal topologies, J. Mech. Phys. Solids 125 (2019) 401–419.

[14] M. F. Ashby, Mechanical properties of cellular solids, Metall. Trans. A 14 (1983) 1755–1769.

[15] L. J. Gibson, M. F. Ashby, Cellular solids: structure and properties, 2 ed., Cambridge University Press, 1997.

[16] J. Y. Chen, Y. Huang, M. Ortiz, Fracture analysis of cellular materials: a strain gradient model, J. Mech. Phys. Solids 46 (1998) 789–828.

[17] F. Lipperman, M. Ryvkin, M. B. Fuchs, Fracture toughness of two-dimensional cellular material with periodic microstructure, Int. J. Fract. 146 (2007) 279–290.

[18] K. Berkache, S. Phani, J.-F. Ganghoffer, Micropolar effects on the effective elastic properties and elastic fracture toughness of planar lattices, Eur. J. Mech. A Solids 93 (2022) 104489.

[19] N. A. Fleck, X. M. Qiu, The damage tolerance of elastic-brittle, two-dimensional isotropic lattices, J. Mech. Phys. Solids 55 (2007) 562–588.

[20] I. Quintana-Alonso, N. A. Fleck, Damage tolerance of an elastic-brittle diamond-celled honeycomb, Scr. Mater. 56 (2007) 693–696.

[21] N. E. Romijn, N. A. Fleck, The fracture toughness of planar lattices: imperfection sensitivity, J. Mech. Phys. Solids 55 (2007) 2538–2564.

[22] I. Christodoulou, P. J. Tan, Crack initiation and fracture toughness of random voronoi honeycombs, Eng. Fract. Mech. 104 (2013) 140–161.

[23] H. Gu, A. Shterenlikht, M. Pavier, Brittle fracture of three-dimensional lattice structure, Eng. Fract. Mech. 219 (2019) 106598.

[24] M. T. Hsieh, V. S. Deshpande, L. Valdevit, A versatile numerical approach for calculating the fracture toughness and R-curves of cellular materials, J. Mech. Phys. Solids 138 (2020) 103925.

[25] H. C. Tankasala, N. A. Fleck, The crack growth resistance of an elastoplastic lattice, Int. J. Solids Struct. 188-189 (2020) 233–243.

[26] J. S. Huang, L. J. Gibson, Fracture toughness of brittle honeycombs, Acta Metall. Mater. 39 (1991) 1617–1626.

[27] I. Quintana-Alonso, S. P. Mai, N. A. Fleck, D. C. Oakes, M. V. Twigg, The fracture toughness of a cordierite square lattice, Acta Mater. 58 (2010) 201–207.

[28] P. E. Seiler, H. C. Tankasala, N. A. Fleck, The role of defects in dictating the strength of brittle honeycombs made by rapid prototyping, Acta Mater. 171 (2019) 190–200.

[29] S. Luan, E. Chen, S. Gaitanaros, Energy-based fracture mechanics of brittle lattice materials, J. Mech. Phys. Solids 169 (2022) 105093.

[30] I. Quintana-Alonso, N. A. Fleck, Fracture of brittle lattice materials: a review, in: I. M. Daniel, E. E. Gdoutos, Y. D. S. Rajapakse (Eds.), Major accomplishments in composite materials and sandwich structures, Springer Netherlands, Dordrecht, 2009, pp. 799–816.

[31] M. Omidi, L. St-Pierre, Fracture toughness of semi-regular lattices, Int. J. Solids Struct. (2023) 112233.

[32] H. C. Tankasala, V. S. Deshpande, N. A. Fleck, 2013 Koiter medal paper: Crack-tip fields and toughness of two-dimensional elastoplastic lattices, J. Appl. Mech. 82 (2015) 1–10.

[33] S. K. Maiti, M. F. Ashby, L. J. Gibson, Fracture toughness of brittle cellular solids, Scr. Mater. 18 (1984) 213–217.

[34] I. Schmidt, N. A. Fleck, Ductile fracture of two-dimensional cellular structures, Int. J. Fract. 111 (2001) 327–342.

[35] H. Gu, M. Pavier, A. Shterenlikht, Experimental study of modulus, strength and toughness of 2D triangular lattices, Int. J. Solids Struct. 152-153 (2018) 207–216.

[36] A. Markou, L. St-Pierre, In-plane mechanical properties of demi-regular lattice materials, Preprint (2023) https://doi.org/10.31224/2956.